Thin Solid Films 519 (2011) 5323–5328

Contents lists available at ScienceDirect

Thin Solid Films

journal homepage: www.elsevier.com/locate/tsf

Effects of Ag doping on the crystallization properties of Sb-rich GeSb thin films

Nam Hee Kim [a], Hyung Keun Kim [a], Kyu Min Lee [a], Hyun Chul Sohn [a], Jae Sung Roh [b], Doo Jin Choi [a,*]

[a] Department of Materials Science and Engineering, Yonsei University, 134 Shinchon-dong, Seodaemun-gu, Seoul 120-752, Republic of Korea
[b] Memory R&D Division, Hynix Semiconductor Inc., San 136-1, Amiri, Bubal-eup, Ichon-si, Gyeonggi-do, 467-701, Republic of Korea

ARTICLE INFO

Article history:
Received 8 April 2010
Received in revised form 27 January 2011
Accepted 8 February 2011
Available online 24 February 2011

Keywords:
Sb-rich GeSb
Ag doping
Phase change
Transmission Electron Microscopy
Static test

ABSTRACT

Ag-doped and un-doped Sb-rich GeSb thin films were deposited by DC magnetron co-sputtering. The electrical, structural, and optical properties of the thin films phase change were investigated using 4-point probe measurement, X-ray diffraction (XRD), transmission electron microscopy (TEM), and a static tester. With increasing Ag doping content, the crystallization temperature and sheet resistance of crystalline state decreased from 325 °C to 283 °C and from 187.33 Ω/□ to 114.62 Ω/□, respectively. XRD patterns of the films showed a Sb hexagonal structure, and the calculated grain size increased from 13.9 nm to 17 nm as the Ag concentration increased. Grain sizes of the Ag-doped thin films were larger than the grain sizes of un-doped thin films, as determined by TEM images. A static tester verified the decreased crystallization speed and optical contrast. Un-doped GeSb crystallization took 160 ns and 16 at.% Ag-doped GeSb crystallization took 200 ns when the laser power was 13 mW. Based on a power–time-effect diagram, the 12.6 at.% Ag-doped GeSb showed good thermal stability in a crystalline state.

1. Introduction

Phase change materials, such as compact disks, digital versatile disks, and blu-ray disks, have been used extensively for optical storage as they store information by optical changes between amorphous and crystalline phases [1]. These phase change materials can also be applied to phase change random access memory (PRAM) technology, which stores the information by the electrical resistivity differences between the two phases.

Recently, PRAM has become a promising candidate for the next generation of non-volatile memory due to its scalability, fast operation speed, and compatibility with the complementary metal–oxide–semiconductor manufacturing process [2]. The most widely adopted phase change material is $Ge_2Sb_2Te_5$ (GST225). However, there are some reports that Te can easily diffuse and interact with adjacent elements, deteriorating the reliability of the PRAM device [3]. Moreover, Te is toxic and, therefore, is not environmentally friendly. In this study, Te-free Sb-rich GeSb was chosen as a phase change material due to the fast crystallization speed as it is a grain growth dominant material [4], with high amorphous phase stability and an adequate archival life time [5] due to high crystallization temperature, as compared to commonly used phase change materials, like GST225 (156 °C), Sb_2Te (114 °C), Ag/In doped Sb_2Te (AIST, 163 °C) [6], and $Ge_1Sb_4Te_7$ (GST147, 150 °C) [7].

Significant work has been performed to improve the operating performance of PRAM by changing the device structure [8], adding a heating layer [9] and doping with various elements, such as N [10], O [11], Sn [12], and Si [13] to phase change the materials. In this work, Ag was chosen as a dopant, as it has already shown improved properties of GST225 [14] and Sb_2Te_3 (ST23) [15] phase change materials containing chalcogen Te elements. However, Ag doping of Te free Ge–Sb phase change materials for PRAM applications have been rarely reported. Sb-rich GeSb was doped with Ag, and the property changes of un-doped Sb-rich GeSb (GS) and Ag-doped GeSb (AGS) thin films were observed. Hereafter, 6.9 at.% Ag-GeSb, 12.6 at.% Ag-GeSb and 16 at.% Ag-GeSb will be represented as 6.9AGS, 12.6AGS and 16AGS, respectively.

2. Experiment

One hundred-nm-thick GS and AGS thin films were deposited by DC magnetron co-sputtering from Ag (99.99%, SMC Tech Co. Ltd., Korea) and $Ge_{20}Sb_{80}$ (99.99%, SMC Tech Co. Ltd., Korea) targets at room temperature on glass and Si(100) substrates. The doped Ag content was altered by 0, 6.9, 12.6, and 16 at.% in the thin films by maintaining the Ag sputtering power at 0, 2.75, 5.6 and 8.55 W, while the sputtering power of $Ge_{20}Sb_{80}$ was maintained at 24 W. The concentration of each element in the film was verified by an electron probe X-ray microanalyzer (EPMA, EPMA 1600). The film thicknesses were measured by a surface profiler AS500 (KLA-Tencor Co.). The base pressure was less than 2.67×10^{-4} Pa (2.0×10^{-6} Torr), and the working pressure was 1.07×10^{1} Pa (8.0×10^{-3} Torr), which was the proper pressure in this study for generating plasma with an Ar flow of

* Corresponding author.
E-mail address: drchoidj@yonsei.ac.kr (D.J. Choi).

0040-6090/$ – see front matter © 2011 Elsevier B.V. All rights reserved.
doi:10.1016/j.tsf.2011.02.031

40 SCCM. A substrate holder was rotated to obtain uniform thickness. In order to crystallize the films, the specimens were annealed by a halogen heater in a chamber at a ramp rate of 10 °C/min in an Ar atmosphere. A 4-point probe (CMT-SR 2000N, Korea) was used to confirm changes in the sheet resistance of each film. The crystal structure was analyzed by X-ray diffraction (XRD, D/MAX-2500H, Rigaku, Japan) using CuKα (λ = 0.15405 nm) radiation with a two-theta range of 20°–55°, in which the main peaks are located. Grain sizes were calculated by the Debye–Scherer formula using the XRD patterns and observed by transmission electron microscopy (TEM, JEM-2100, JEOL) images using a 0.00197 nm of electron wavelength. A static tester (Nanostorage Co. Ltd., Korea) was conducted by laser irradiation (λ = 650 nm) in the nanosecond temporal scale in order to observe the crystallization behavior.

3. Results and discussion

Fig. 1 shows the EPMA result of GS and AGSs. The x-axis represents the Ag sputtering power, and the y-axis represents the concentration of each element. The concentration of the sputtered GS thin film was similar to the target composition of $Ge_{20}Sb_{80}$. The Ag doping concentration increased with increasing Ag sputtering power, and the ratio of Ge:Sb was maintained as 1:3.09–3.26. The error bar was indicated at each concentration point in Fig. 1, and the standard deviation of the concentration was approximately ±1.6 at.%. Therefore, this EPMA result was pretty reliable.

Fig. 2a shows the sheet resistance as a function of the temperature for GS and AGS thin films. The films were annealed at each temperature point for 20 min at a ramp rate of 10 °C/min. The sheet resistance was high at the lower annealing temperature and abruptly decreased after a specific annealing temperature, likely due to film crystallization. The sheet resistance and crystallization temperature in the amorphous and crystalline states decreased as the Ag doping content increased in the films. For more specific analysis, the changes in resistance of the crystalline state, the set state (R_{set}), and crystallization temperature were shown in Fig. 2b and c. The average sheet resistance in the crystalline state, R_{set}, was 187.33 Ω/□, 158.98 Ω/□, 116.14 Ω/□ and 114.62 Ω/□ for GS, 6.9AGS, 12.6AGS, and 16AGS, respectively. In order to define the crystallization temperature, the sheet resistance graph was differentiated, and the minimum value of the derivative of each graph was regarded as the crystallization temperature. The crystallization temperature was approximately 325 °C, 315 °C, 288 °C, and 283 °C for GS, 6.9AGS, 12.6AGS, and 16AGS, respectively. The decreased crystallization temperature by doping Ag can be explained by a total bond enthalpy. Lankhorst [16] reported that the glass transition temperature corresponded to the total bond enthalpy, which was mostly related to the bond enthalpy and the number of bonds between atoms. The bond

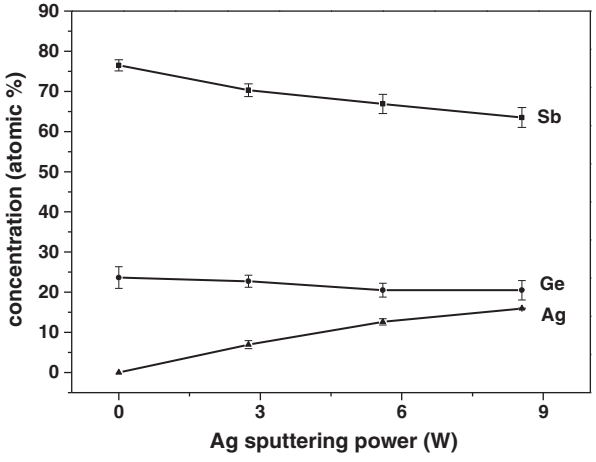

Fig. 1. EPMA results of each element as a function of the Ag sputtering power.

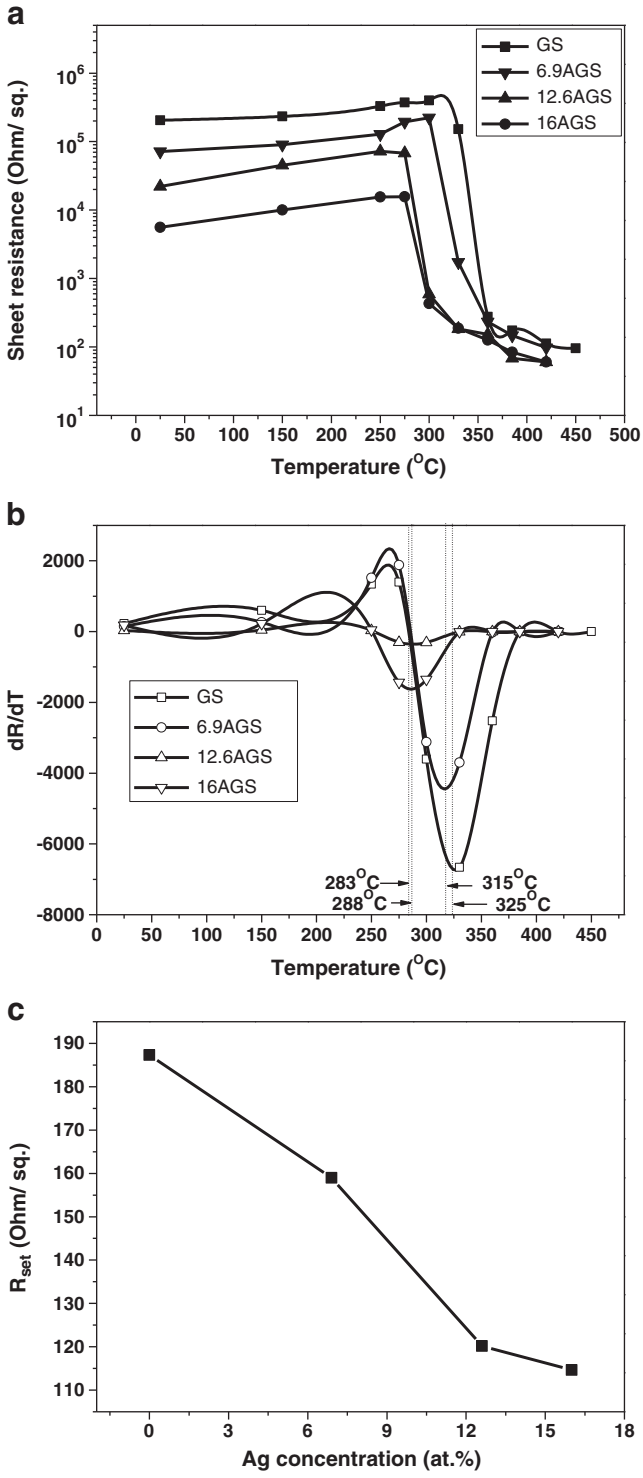

Fig. 2. (a) Sheet resistance changes as a function of temperature, (b) average sheet resistance in the crystalline state (R_{set}), and (c) differentiated sheet resistance change as a function of temperature for GS, 6.9AGS, 12.6AGS, and 16AGS.

enthalpy of Ag–Ag is −50 kJ/mol, which is the average of the two values in Ref. [16]. This value was too low, compared to the bond enthalpies of Ge–Ge (186 kJ/mol) and Sb–Sb (175 kJ/mol) [16]. Therefore, AGS has a low glass transition temperature since the Ag atom leads to a low, total bond enthalpy. We also calculated glass transition temperature in accordance with the equations from the paper of Lankhorst. The crystallization temperature can be determined by experimental fact that the glass transition temperatures of the materials are mostly 80% of the